International Journal of Nanomedicine

Dovepress
open access to scientific and medical research

Open Access Full Text Article

REVIEW

Hypoxia-active nanoparticles used in tumor theranostic

This article was published in the following Dove Press journal:
International Journal of Nanomedicine

Yaqin Wang[1,2,*]
Wenting Shang[2,*]
Meng Niu[1]
Jie Tian[2,3]
Ke Xu[1]

[1]Department of Interventional Radiology, The First Affiliated Hospital of China Medical University, Shenyang, People's Republic of China; [2]Chinese Academy of Sciences Key Laboratory of Molecular Imaging, Institute of Automation, Chinese Academy of Sciences, Beijing 100190, People's Republic of China; [3]Institute of Medical Interdisciplinary Innovation, Beihang University, Beijing, 100080, People's Republic of China

*These authors contributed equally to this work

Abstract: Hypoxia is a hallmark of malignant tumors and often correlates with increasing tumor aggressiveness and poor treatment outcomes. Therefore, early diagnosis and effective killing of hypoxic tumor cells are crucial for successful tumor control. There has been a surge of interdisciplinary research aimed at developing functional molecules and nanomaterials that can be used to noninvasively image and efficiently treat hypoxic tumors. These mainly include hypoxia-active nanoparticles, anti-hypoxia agents, and agents that target biomarkers of tumor hypoxia. Hypoxia-active nanoparticles have been intensively investigated and have demonstrated advanced effects on targeting tumor hypoxia. In this review, we present an overview of the reports published to date on hypoxia-activated prodrugs and their nanoparticle forms used in tumor-targeted therapy. Hypoxia-responsive nanoparticles are inactive during blood circulation and normal physiological conditions but are activated by hypoxia once they extravasate into the hypoxic tumor microenvironment. Their use can enhance the efficiency of tumor chemotherapy, radiotherapy, fluorescence and photoacoustic intensity, and other imaging and therapeutic strategies. By targeting the broad habitats of tumors, rather than tumor-specific receptors, this strategy has the potential to overcome the problem of tumor heterogeneity and could be used to design diagnostic and therapeutic nanoparticles for a broad range of solid tumors.

Keywords: prodrug, tumor microenvironment, metal complex, bioreductive

Introduction

The imbalance between the rapid rate of tumor growth and blood supply leads to an insufficient oxygen concentration in aggressively proliferating tumors, which produces a markedly hypoxic intratumor microenvironment.[1–3] More specifically, hypoxia created because of the rapid proliferation and metastatic rates of tumor cells, which increases oxygen consumption. While limited oxygen supply counts on the bad angiogenesis of solid tumor, leading to the intratumoral hypoxia. As a tumor proliferates, hypoxia-inducible factor-1 alpha (HIF-1α) can be upregulated which promotes the production of vascular endothelial growth factor (VEGF) via the HIF-1α signaling pathway, which stimulates the growth of blood vessels. However, the malformed neovascular structure is unable to rescue the oxygen supply because of the low efficiency of the elevated blood circulation. Normal tissue has a molecular oxygen (O_2) level of 2% to 9% (40 mm Hg). In contrast, "hypoxia" and "anoxia" in a tumor microenvironment are defined as O_2 levels of 0.02% to 2% (<2.5 mmHg pO_2).[4–6] Besides, tumor cells are better sustainable in hypoxia via an upregulated HIF-1α pathway, which can transform the glucose metabolism pathway.[7] On the other hand, hypoxia is also correlated with poor

Correspondence: Ke Xu
Department of Interventional Radiology, The First Affiliated Hospital of China Medical University, No.155 Nanjing North Street, Heping District, Shenyang, Liaoning Province 110000, People's Republic of China
Email kexu@sina.vip.com

Jie Tian
Beijing Key Laboratory of Molecular Imaging, Zhongguancun East Road #95, Haidian Dist., Beijing, 100190, People's Republic of China
Email jie.tian@ia.ac.cn

http://doi.org/10.2147/IJN.S196959

overall survival that results from the induction of chemoresistance and radioresistance via the maintenance of noncycling cancer stem-like cells.[8] Hypoxia is a crucial factor in cancer relapse because of its effects on the regulation of the cell cycle, evasion of apoptosis, maintenance and quiescence of stem cells, and selection of treatment-resistant noncycling cancer cells.[9–11]

Overcoming hypoxia is thus an important strategy in the treatment of solid cancers. To this end, studies have sought to develop functional molecules and nanomaterials that can be used to noninvasively image and efficiently treat hypoxic tumors. Three prominent strategies are anti-hypoxia agents, hypoxia-active nanoparticles, and hypoxia-targeting agents. The goal is to reverse hypoxia by producing O_2, and activate the nanoparticles or agents in the hypoxic tumor microenvironment and to target biomarkers of tumor hypoxia to improve the efficacy of the drugs that are administered. Anti-hypoxia agents refer to oxygen generation or oxygen carrier materials, such as MnO_2 and hemoglobin-based O_2 carriers, which can alleviate tumor hypoxia and thus increase the effect of the therapy or reduce malignancy of the tumor. The oxygenation strategy is limited by cytotoxicity, lower blood circulation, and poor penetration within a tumor. On the other hand, concerning the increased level of HIF-1, the unfolded protein response, and mTOR pathways in hypoxia, Hypoxia-targeting agents were designed to imaging and treat hypoxia. Hypoxia-active prodrugs (HAPs, also known as bioreductive prodrugs) can be activated by reducing agents or light-triggered electronic transfer in the tumor microenvironment. Due to the Warburg effect, the metabolism of cancer cells tends to be via aerobic glycolysis rather than the efficient oxidative phosphorylation pathway, which leads to an accumulation of reducing agents and oxidoreductases, such as NADH or NADPH, cytochrome P450 reductase, DT-diaphorase, nitroreductase, alkaline phosphatase, and β-glucuronidase.[12] Typically, HAPs can be reduced by the aforementioned enzymes into a radical anion intermediate through one-electron or two-electron oxidoreductases pathways. In aerobic tissues, back-oxidation of the radical anion to the starting drug is kinetically favored. In contrast, in an oxygen-poor environment, the extended lifetime of the radical anion intermediate enables metabolic reactions that convert the parent drug to a cytotoxic agent.[13] This reversible step ensures that prodrug activation is restricted to tissues with limited oxygen availability, resulting in hypoxia-selective cell death. Two-electron reduction by certain oxidoreductases fails to generate an oxygen-sensitive radical intermediate. In this case, drug sensitivity is determined by the ability of oxygen to reverse the activation process and the overexpression of oxidoreductases in tumor tissues.

The earliest discovery of prodrugs can be traced to the 1960s with the discovery of the DNA cross-linking anticancer antibiotic mitomycin C (MMC), which is activated by reduction of its indoloquinone moiety.[14,15] In the 1970s, it was proposed that hypoxia could be advantageous for therapeutics, prodrugs could be metabolized to a cytotoxic compound only in hypoxic cells. Many bioreductive drugs have been reported to date. This HAPs would provide a specific method of killing treatment-resistant cells with no to little systemic toxicity. Drugs based on the presence of quinones (Table 1), nitro-groups (Table 2), aromatic N-oxides (Table 3), aliphatic N-oxides (Table 4), and transition metals (Table 5) have been widely applied in hypoxia-responsive systems. However, despite advances in HAPs for tumor therapy, a small molecular drug is rapidly cleared through renal filtration. This reduces the drug's lifetime in the circulatory system, which leads to ineffective levels of the drug in tumors. Moreover, the systemic toxicity of these drugs, which includes neurotoxicity and myelotoxicity, has restricted the clinical application of these drugs. Compounds used as drugs need to have potent bioactivities and should have a long blood circulation time and high biocompatibility. As well, there should be few side effects. To achieve this goal, researchers have combined these HAPs with microenvironmental targeting antigen/proteins to elevate the tumor targeting efficiency, vascular endothelial growth factor (VEGF), carbonic anhydrase IX, and biotin have been used.[16,17] And materials that are nanocrystallized and modified can persist in the circulation and can be highly biocompatible. These effective nanoparticles can undergo redox-based structural changes or oxygen concentration based electronic conversion, which can permit simultaneous diagnosis and treatment in the hypoxic tumor microenvironment, such as the use of fluorescence, phosphorescence or photoacoustic imaging, and chemotherapy or radiotherapy.[18,19] Nanocarriers have proven to be better-targeted delivery options that are capable of uploading and releasing HAPs and other drugs within the tumor microenvironment that have the advantages of longer circulation time, better tumor penetration, and greater drug accumulation. However, hypoxia-active nanoparticles have limitations that include the low efficiency of extravasation

Table 1 Typical samples of quinone

Chemical types	Agent	Application	Mechanism of action	Activating enzyme	References
Quinones	Mitomycin C	Chemotherapy	DNA alkylation oxidative stress	CPR, DTD	101
	Porfiromycin	Chemotherapy	DNA crosslinking	CPR, DTD	54
	EO9 (Apaziquone)	Cancer therapy	DNA alkylation oxidative stress	CPR, DTD	52,102
	Indolequinone	Chemotherapy	Alkylating agent	CYP, NQO1	103
	Aziridinylbenzoquinones (AZQ;NSC 182986)	Chemotherapy	Alkylating activity	DTD, CPR	53,104,105

Table 2 Typical samples of nitro derivatives

Chemical types	Agent	Application	Mechanism of action	Activating enzyme	References
Nitro derivatives	Nitroimidazoles	Chemotherapy Radiosensitizer	DNA damage	Reduce by many bioreducing agents	39,106
	Etanidazole(SR-2508)	Radiosensitizer chemotherapy	Alkylating DNA and prevent DNA repair	Nitroreductases	107,108
	Misonidazole	Radiosensitizer	DNA alkylating agents	Nitroreductases	109
	Pimonidazole	Imaging	Immunohistochemistry	Nitroreductases	110
	Sanazole (AK-2123)	Radiosensitizer	Complex DNA damage	CYP	111
	Nimorazole	Radiosensitizer	Complex DNA damage		112,113
	plus tretazicar (CB 1954)	Chemotherapy	Complex DNA damage	Nitroreductases and DTD	114
	RSU 1069 and RB 6145	Radiosensitizer Chemotherapy	Complex DNA damage	nitroreductases	115
	Evofosfamide (TH302)	Chemotherapy	alkylating DNA	Nitroreductases	116–118
	PR-104	Chemotherapy	DNA crosslinking	CYPOR	119,120
	KS119	Radiosensitizer	Alkylate the O(6)-position of guanine in DNA	Nitroreductases	121,122
	NLCQ.1(NSC 709257)	Chemotherapy Radiosensitizer	Complex DNA damage	CYP and b(5) reductases	123–125
	CI-1010	Chemotherapy Radiosensitizer	Alkylating DNA in chemotherapy, Complex DNA damage as radiosensitizing	Unknown	126,127
	RH1	Chemotherapy	DNA cross linking	DTD	128,129
	SN23862	Chemotherapy	Complex DNA damage	CYPOR	130,131

Table 3 Typical samples of aromatic N-oxides

Chemical types	Agent	Application	Mechanism of action	Activating enzyme	References
Aromatic N-oxides	quinoxaline 1,4-dioxides (QdNOs)	Chemotherapy	Reduce hypoxia-induced gene expression.	Unknown	132
	SN30000 (CEN-209)	Chemotherapy	Complex DNA damage	CYPOR, MTRR, NOS2A and NDOR1	133–137
	TPZ (tirapazamine,SR 4233)	Chemotherapy	Complex DNA damage	CYPOR, DTD	138

into the deeper regions of a tumor, due to their relatively large size compared to small chemical prodrugs, which is more effective than the enhanced permeability and retention effect. Besides, drug loading and release efficiency of the nanoparticles is still handicap in clinical application. In this review, we describe the recent progress and the development of HAP nanoparticles in tumor theranostics and their advantages and drawbacks.

Table 4 Typical samples of aliphatic N-oxide

Chemical Types	Agent	Application	Mechanism of action	Activating enzyme	References
Aliphatic N-oxide	AQ4N (Banoxantrone)	Chemotherapy Radiosensitizer and Imaging	Topoisomerase II inhibitor	CYP, NOS	139
	OCT1002	Chemotherapy Radiosensitizer and Imaging	High affinity for DNA and targeting of topoisomerase II	CYP	140

Table 5 Typical samples of metal complexes

Chemical types	Agent	Application	Mechanism of action	Activating enzyme	References
Metal complexes	Cobalt (III) complex	Phosphorescent	Transition metal ions	Reducing agent	141
	Platinum (IV)	Phosphorescent	Transition metal ions	GSH, Ascorbate, NAD(*P*)H, and Cysteine-containing proteins	142
	Ruthenium (III)	Phosphorescent	DNA binding	GSH, Ascorbate	143
	Cu (II)	Radiosensitizer	Generate ROS	Reducing agent	144

Abbreviations: CYP, cytochrome P450; DTD, DT-diaphorase, CYPOR, NADPH–cytochrome P450 reductase; ICL, DNA interstrand crosslink; TOPOII, topoisomerase II; MTRR, methionine synthase reductase; NOS2A, inducible nitric synthase; NDOR1, novel diflavin oxidoreductase; iNOS, inducible nitric oxide synthase; GSH, glutathione.

Hypoxia-active nanoparticles for imaging

Hypoxia-active fluorescence nanoparticles

Azobenzene

Fluorescence imaging for nanoparticles has been developed over several decades since the late 1980s. Several optical probes have been developed by employing nitroaromatic, quinone, or azobenzene derivatives as hypoxia-sensitive moieties based on the hypoxia-triggered molecular cleavage of these derivatives. A representative example for these probes is azobenzene compounds, which can serve as an alternative to the commonly used nitrobenzene and nitroimidazole-based hypoxia-activated triggers. Azobenzene compounds can be reduced stepwise by nicotinamide adenine dinucleotide phosphate (NADPH) and quinone reductase 1 (NQO1, a cytosolic reductase up-regulated in many human cancers) in the critically required hypoxic environment of tumor cells. Piao et al[20] proposed the use of novel fluorescent azobenzene-based seleno-rosamine dye conjugated probes obtained by chemically attaching azobenzene compounds with 2-methyl (2Me) Rhodamine Green (2Me RG) and 2Me Si-rhodamine600 (2Me SiR600) to form mono-azo rhodamine and mono-azo Si-rhodamine, respectively. Both these compounds can be activated as fluorescence and photosensitizer probes during mild hypoxia, owing to the reductive cleavage of the azobenzene group. These hypoxia-active fluorescence probes are very sensitive and selective to hypoxia at oxygen concentrations up to approximately 5%. In this study, azobenzene compounds served as fluorescence quenchers as well as activators. Although the applications of these HAPs as nanoparticles in the single fluorescence mode are limited, many researchers have applied them by using these compounds in MRI, CT, and photoacoustic imaging, and even in therapy.

Cobalt

Cobalt (Co) is relatively abundant and inexpensive and is essential for the metabolism of all animals. A number of cobalt complexes have been explored as HAPs. In general, Co(III) complexes are highly inert. Upon bioreduction, the complexes are reduced to their more labile Co(II) forms. Co(II) complexes re-oxidize to Co(III) complexes in the presence of O_2 in normal tissue. In hypoxic environments in the presence of endogenous reductases, such as P-450 and xanthine oxidase, the labile Co(II) forms can dominate, allowing structure change to release the drug. This fine-tuning has inspired the synthesis of a variety of promising hypoxia-selective prodrug frameworks. Yamamoto et al documented the delivery of a fluorescent coumarin using a Co(III) chaperone to target hypoxic regions. Fluorescence tagging of Co(III) compounds is an effective

and noninvasive method for monitoring ligand release and the subsequent cellular accumulation and localization of the cytotoxin. This selective accumulation and monitored activation in tumor microenvironments can minimize the toxicity of anticancer drugs, as well as imaging hypoxia.[21]

Hypoxia-active phosphorescent nanoparticles

In addition to the aforementioned fluorescent nanoparticles, which are activated based on the redox degree of the cells, phosphorescent transition metal (PTM) complexes can directly sense O_2 concentrations[22] based on characteristics that include lower excitation energy, longer emission time, and deeper penetration, compared with fluorescence imaging. Normally, the PTM complexes exist in the ground state. Upon photoexcitation, PTMs absorb photons and reach the excited single state (S_1). Then, through the processes of internal conversion and intersystem crossing, they quickly relax to the excited triplet state (T_1) and emit phosphorescent light. Quenching can occur in the presence of O_2, which reduces the yield and lifetime of the phosphorescence in a concentration-dependent manner. It is generally considered that the ground state O_2 molecule accepts energy from the excited triplet state of PTM to yield excited states $^1\Delta g$-Σg^+ of O_2 (Figure 1D). PTM complexes, which include iridium (III) and ruthenium (II) complexes, and platinum (II) and palladium (II) porphyrins (Figure 1A–C), have been employed to sense and image the O_2 levels in living organisms. These complexes are reversibly dependent on the changes in O_2 concentration and hence can function as real-time O_2 monitors.[23–26]

Iridium(III) complexes

Iridium(III) complexes are typical PTM complexes, which exhibit intense and long-lived phosphorescence. The phosphorescence of iridium(III) complexes is quenched by the intracellular O_2, which is restored through two-electron bioreduction in a hypoxic environment. Wen et al[27] synthesized an oxygen-sensitive complex, with iridium covalently attached to mesoporous silica-coated and core-shell upconverted nanoparticles (UCNPs), denoted as core-shell UCNPs@mSiO_2-Ir, to monitor O_2 concentrations as indicated by the increase or decrease in through luminescence. The up-conversion channel of iridium can emit 600 nm oxygen-quenchable phosphorescence after absorbing 980 nm near-infrared (NIR) light, which is converted from the energy of UCNPs, and hence, can exhibit relatively deep tumor penetration compared with non-NIR light excitation. The down-conversion channel of iridium exhibits the reduction in long-lived oxygen-sensitive phosphorescence of the nanoprobe from 4.0 to 0.8 μs when the transformation from hypoxia into normoxia. This is advantageous since short-lived autofluorescence can be eliminated via time-gated luminescence imaging technology by exerting an appropriate delay time to enhance the signal-to-noise ratio. The complex iridium exhibits intense and long-lived phosphorescence that is highly sensitive to oxygen quenching. Both the channels were adopted to remove the possible interference from background autofluorescence. Moreover, Wen et.al.[28] also designed two iridium (III) complexes that specifically stain the mitochondria (Ir-P(ph)3) and lysosomes (Ir-alkyl) in living cells, respectively. These complexes exhibited similar photophysical properties and singlet oxygen quantum yields due to the same cyclometallic ligands. Mitochondria-targeted Ir-P(ph)3 could lead to an improved PDT effect compared to the lysosome-targeted complex, especially during hypoxia, indicating the practical potential of mitochondria-targeted PDT agents in cancer therapy. Feng et al[29,30] synthesized negatively charged hyperbranched phosphorescent conjugated polymer dots with the iridium(III) complex as the core for imaging of hypoxia and highly efficient PDT. In the formulation, oxygen-insensitive blue fluorescent 9, 9-dioctylfluorene forms the backbone of the hyperbranched conjugated polymer and oxygen-sensitive red phosphorescent iridium (III) complex forms the core of this polymer. Upon decreasing the O_2 content from 21% to 2.5%, the red emission intensity of iridium(III) complex collected at 600 to 700 nm showed remarkable enhancement, while the intensity of blue emission from polyfluorene moieties at 420 to 490 nm remained unchanged under various contents of O_2. By calculating the ratio of intensity of emission at 600 to 700 nm and that at 420 to 490 nm, the actual O_2 contents in the living cells could be obtained. Considering the long phosphorescence lifetime property of this probe, the authors also applied photoluminescence lifetime imaging and time-gated luminescence to improve the signal-to-noise ratios. Thus, Feng et al[29,30] reported the first small molecular probe with iridium(III) complexes, which permitted radiometric imaging, photoluminescence lifetime imaging and time-gated luminescence imaging for hypoxia.

Ruthenium

Although iridium-based probes have the potential to image physiological hypoxia, most have very poor water solubility.

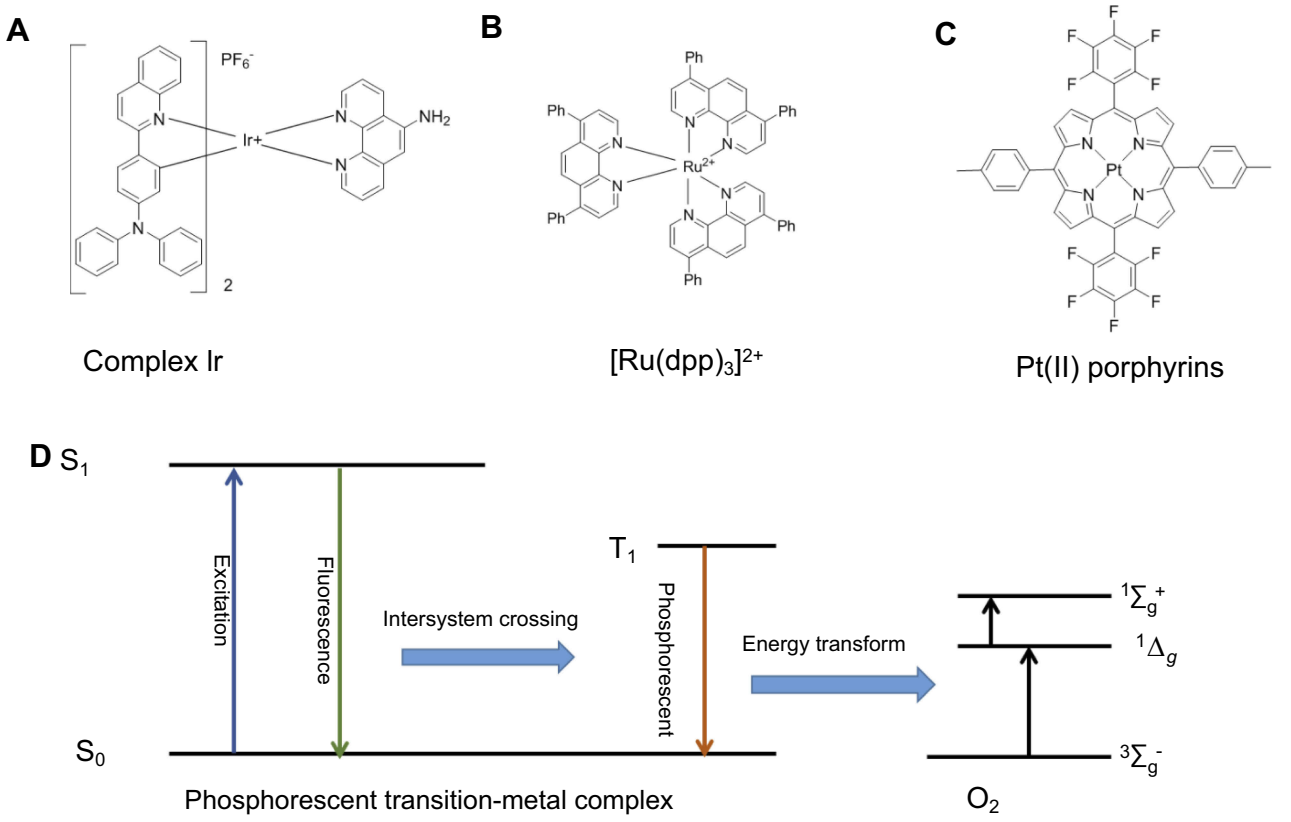

Figure 1 Structure and activation of metal complex. (**A**) complex Ir, (**B**) $[Ru(dpp)_3]^{2+}$ (**C**) Pt(II) porphyrins (**D**) Oxygen sensing mechanism of conjugated polyelectrolyte and schematic illumination of energy level of the moieties in phosphorescent transition-metal S_0, ground state, S_1- excited singlet states by fluorescence light, T_1- triplet state form by S_1 intersystem crossing, $1\Delta_g$-$1\Sigma g+$.

Organic solvents or other solubilizing agents are needed for biological applications. Ruthenium complexes show good water solubility and a strong phosphorescence emission in hypoxia. Liu et al[31] designed UCNP core/hollow mesoporous silica shell-structured nanoparticles with oxygen indicator ruthenium (II) dichloride ($[Ru(dpp)_3]^{2+}Cl_2$). The oxygen indicator for the detection of hypoxia and UCNP provides the excitation light to $[Ru(dpp)_3]^{2+}Cl_2$ by the up-conversion luminescence process at 980 nm. Based on the principle that lanthanide-doped UCNPs can be used as energy donors for up-conversion luminescence resonance energy transfer, but have no oxygen recognition capability by themselves, $[Ru(dpp)_3]^{2+}Cl_2$ was chosen as the quenchable indicator to sense oxygen because its maximum absorbance at 463 nm strongly overlaps with the two emission wavelengths (450 and 475 nm) of UCNPs, and $[Ru(dpp)_3]^{2+}Cl_2$ cannot be directly photoexcited by NIR light. More importantly, the red luminescence of $[Ru(dpp)_3]^{2+}Cl_2$ at 613 nm can be strongly quenched by oxygen,[32] since the concentration of oxygen species could be reflected by the luminescence at 613 nm upon excitation by 980 nm laser. Notably, both external excitation and emission (980/613 nm) are within the ''optical window'' of the biological tissues,[33] which can enable deep tissue imaging.

Platinum(II) porphyrin

Since the approval of cisplatin for cancer therapy in the late 1970s, a number of analogs designed to minimize nephrotoxicity and gastrointestinal toxicity induced by cisplatin have been explored. Up to now, three platinum (Pt)(II) complexes have received Food and Drug Administration (FDA) approval: cisplatin, carboplatin, and oxaliplatin. In routine use worldwide, the FDA approved Pt(II) cancer drugs have proven to be far from ideal. Based on this fact, a series of hydrophilic phosphorescent starburst Pt(II) porphyrins as bifunctional therapeutic agents for simultaneous tumor hypoxia imaging and highly efficient PDT have been rationally designed and synthesized. Researchers have constructed Pt(II) porphyrins with excellent photophysical properties, such as high photostability, large Stokes shift, long phosphorescence emission lifetime, and deep-red emission. By introducing phosphorescent Pt(II) porphyrin (O_2-sensitive) into a fluorene-based conjugated polyelectrolyte (O_2-insensitive),

Pt(II) porphyrins exhibit excellent radiometric luminescence response to O_2 levels with high reliability and full reversibility. Pt(II) porphyrins have been used widely as oxygen probes that combine fluorescence and phosphorescence into a single nanoprobe.[34,35] Another study described that Pt(II) porphyrin can act as an oxygen-responsive phosphorescent group and $^1O_2$ photosensitizer upon conjugation to a polyfluorene-based hyperbranched polyelectrolyte to increase biocompatibility and water solubility. For early-stage diagnosis and therapy systems, Pt(II) porphyrin show a high PDT efficiency and longer lifetimes, and higher signal-to-noise ratio in fluorescence detection.[36]

Hypoxia-active positron emission tomography (PET) imaging probe

Copper (Cu) (II) complexes

Cu(II) complexes as a hypoxic cell sensitizer can be reduced to form Cu(I) complexes with reduced stability to release an active ligand. The redox reaction is closely correlated with cell toxicity. Cu(ll)-diacetyl-bis(A/4-methylthiosemicarbazone) (Cu-ATSM) that features pronounced membrane permeability and low redox potential was evaluated as a possible hypoxia imaging agent.[60] Cu-ATSM has the same range of redox potential as NADH, which can accumulate in a hypoxic compartment by the same reductive retention mechanism as cobalt.[37]. Furthermore, radioactive isotopes of Cu can be used, which permits radiation therapy to be used in combination with bioreduction.[62] Cu-ATSM is a very promising radiopharmaceutical for the PET imaging of hypoxic tumors. As described by Fujibayashi et al,[37,62] Cu-ATSM uptake depends on an intracellular cytosolic/microsomal bioreduction processes. Lopci et al[62] described the use of Cu-ATSM to image hypoxia in non-small cell lung cancer. The advantages of this approach included rapid target accumulation that was dependent on the oxygen level. Increased tumor-to-background signal assures tumor delineation, especially for advanced tumors targeted for exclusive radiation therapy or in combination of chemoradiation.[38] The results echo those obtained with the imaging using 18F-fluorodeoxyglucose.

Hypoxic-active nanoparticles as radiosensitizers

Nitroimidazoles

Nitroimidazoles are the most frequently used HAPs, and they have been evaluated in phase II clinical trials. They display multiple bioactivities and have been used in cancer treatment since the 1950s.[39,40] Nitroimidazoles can be reduced into an amine derivative or hydroxylamine through one-electron reduction[41] by a series of nitroreductases coupled with bioreducing agents in the absence of adequate supply of oxygen. This step is reversible under normal O_2 levels due to higher electron affinity of O_2 than the nitro group (Figure 2A).[42] Thus, this oxygen-dependent oxidation confers hypoxia sensitivity to the nitroimidazole analogs. As a sensitive agent, the analogs have slight or no drug effect on their own. Their use in combination with many imaging and therapeutic agents can allow multimodal imaging and therapy. In recent years, researchers have developed various nanoparticles containing nitroimidazoles. Liu et al.[43] prepared a hypoxic radiosensitizer prodrug with doxorubicin liposome that was used for combined radiotherapy and chemotherapy of malignant gliomas. Hypoxic radiosensitizer nitroimidazoles have been conjugated with lipid molecules with a hydrolyzable ester bond to form nitroimidazole molecules. The molecules were mixed with 1,2-distearoyl-sn-glycero-3-phosphoethanolamine-N-[amino(polyethylene glycol)-2000] and cholesterol to produce liposomes enclosing the MLP prodrug. The liposomes displayed strong radiosensitivity and promoted the nitroimidazole-mediated release of the prodrug cargo under hypoxic conditions.

In addition to the tumor regions, many other hypoxic regions exist. These regions include bone marrow.[44] Intelligent delivery systems that are responsive to a single internal or external stimulus often lack sufficient cancer selectivity, which compromises drug efficacy and induces undesired side effects. To overcome these limitations, two strategies have been used recently to improve the selectivity of drug release. Lin et al[45] introduced a novel strategy for drug delivery by integrating both internal and external controls. The internal control used tumor hypoxia to unlock the drug delivery system. The external control employed photoactivation to release the drug payload upon excitation by either one-photon visible light or two-photon NIR light. Nitroimidazole was incorporated into the coumarin phototrigger as an electron acceptor and a sufficiently high two-photon absorption cross section (Figure 3). In aerobic tissues, any photoexcitation of the coumarin dye relaxes via photoinduced electron transfer to the nitroimidazole electron acceptor, resulting in an absence of fluorescence and photocleavage, and lack of toxicity to normal cells. Conversely, in anaerobic solid tumors, the hypoxia-specific nitro-to-amino reduction activates the coumarin phototrigger. Consequently,

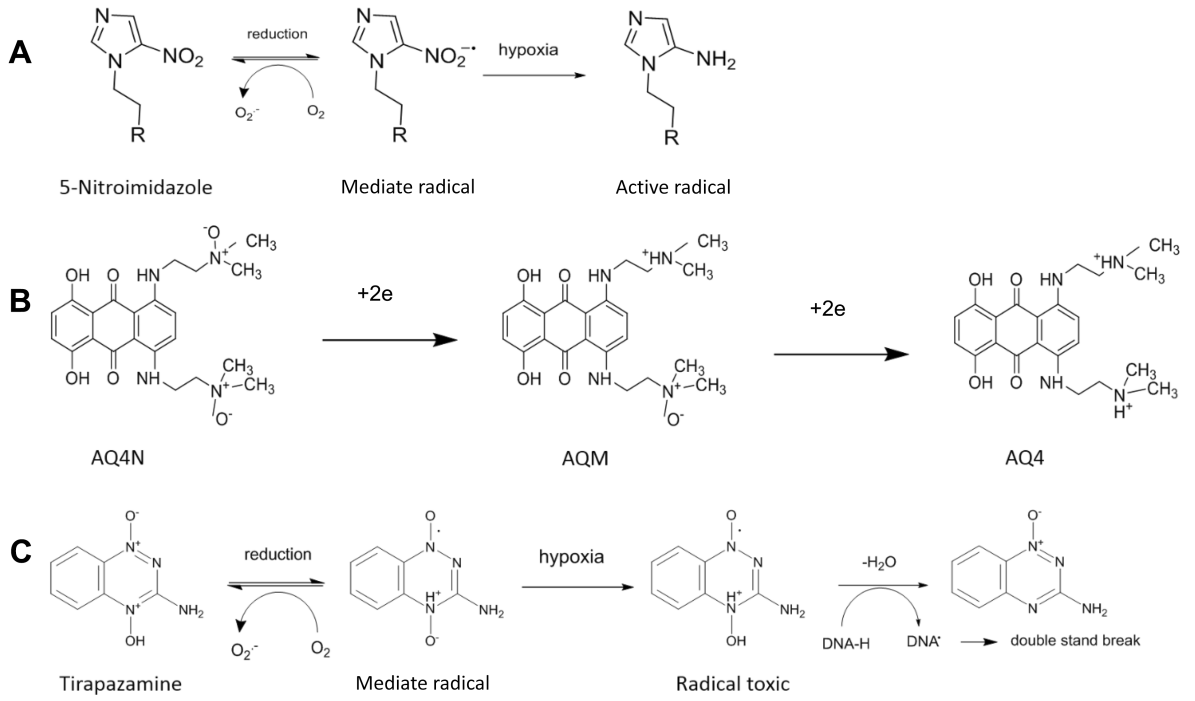

Figure 2 Activation mechanical of HAP. (**A**) 5-Nitroimidazole reduced through one electron pathway. (**B**) AQ4N reduced through two electron pathway (**C**) Tirapazamine reduced through one electron pathway to form DNA toxic.

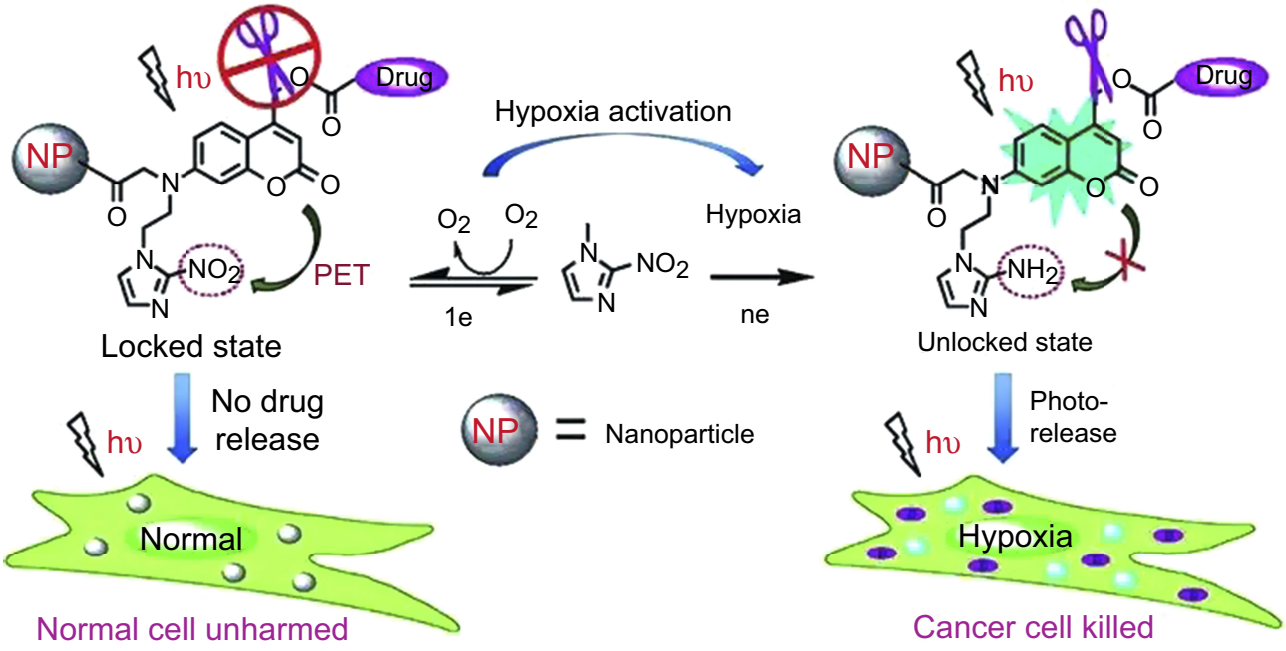

Figure 3 The hypoxia-activated phototrigger specifically releases drug to tumor cells.

photoactivation generates blue fluorescence and causes water-assisted photoheterolysis of the C-O bond to release the caged anticancer drugs for cancer treatment. However, the clinical application of this formulation is hampered by the limited tissue penetration depth of light. To circumvent this limitation, Liu et al[46] developed an X-ray responsive nanosystem composed of PEGylated gold nanoparticles with conjugated nitroimidazole and cell-penetrating peptides that combined active hypoxia and X-ray stimuli. The reactivity of the nanoparticles can be remotely controlled by X-rays.

Due to its excellent stability, the PEGylated gold nanoparticles could potentially decrease radiotherapy toxicity, allowing radiosensitization at the target site receiving the highest dose during radiotherapy. These properties have been demonstrated in vitro using a clinically relevant X-ray source on resistant hypoxic cells, suggesting potential applications of such nanosystems in cancer radiotherapy.

Sanazole

Sanazole (SAN) is a nitrotriazole compound. It is a potent hypoxic cell radiosensitizer, which has completed phase III clinical trials, which demonstrated significant increases in local tumor control and survival.[47] The mechanism of sensitization is ascribed to the bioactivation through xanthine oxidase and microsomal NADPH/cytochrome P450 reductase, leading to increased DNA damage.[48] Sreeja et al[49] composed a nanoparticle formulation containing chemotherapeutic doxorubicin, iron oxide nanoparticles (Fe_3O_4 NP), together with a hypoxic cell radiosensitizer (SAN) for specific targeting to the tumor sites.[50] This complex can specifically target the tumor site, thereby enhancing the efficacy of doxorubicin. Sreeja et al[49] further confirmed the radiosensitizer properties of SAN, berberine (BBN), and iron oxide nanoparticle complexes (NP-BBN-SAN). The NP-BBN-SAN complexes were more effective in reducing tumor volumes compared to other treatments. The treatment efficacy reflected the activation of apoptosis via caspase-8. Analysis of the transcriptional expression levels of the *HIF-1α, VEGF, AKT, BAX, BCL2, CASPASE 3, CASPASE 8, CASPASE 9*, and *TNF*-α genes in tumor tissues of all the groups revealed a downregulation in the transcript levels of *HIF-1α* and its associated genes, *VEGF* and *AKT*, thereby resulting in tumor regression and activation of TNF-α-induced extrinsic pathway of apoptosis via caspase 8, although other apoptotic pathways also might also be involved.

Hypoxia-active nanoparticles for chemotherapy

Quinones

Prodrugs structurally composed of quinones can also be used as HAPs. The quinone containing structures can be selectively activated by the hypoxic environment in tumor cells to produce semiquinone radicals or by the two-electron reducing enzyme DT-diaphorase to hydroquinones. Natural and synthetic compounds containing a quinone core structure are an important class of biologically active agents and include coenzyme Q, Vitamin K, and the anticancer compound doxorubicin. The quinones that have been used as HAPs include mitomycin C (MMC),[51] EO9,[52] AZQ,[53] and porfiromycin.[54] Among these, MMC has been intensively investigated. MMC was isolated from *Streptomyces caespitosus* in the 1950s. It is very soluble and was the earliest clinically used quinone-containing drug recognized as a bioreductive and hypoxia-selective alkylating agent. It is distributed into nuclei after cellular uptake and intracellular drug delivery. MMC and its analogs produce their cytotoxicity through a reductive metabolism,[55] which crosslinks DNA with high efficiency and absolute specificity for the sequence CpG. While MMC is associated with a number of acute and chronic toxicities, such as irreversible myelosuppression and hemolytic uremic syndrome, which limit its clinical application. Hou et al[56] developed a new method to synthesize MMC-soybean phosphatidylcholine (MMC-SPC) nanoparticles. By taking advantage of enhanced chemical activity of MMC in hypoxic environments. Hou et al[57] further developed MMC-loaded phytosomes with improved formulation characteristics, which included smaller size, lower size distribution, higher zeta potential, and better stability. Zhang et al[58] developed the first two-photon fluorescent probes with two different kinds of mechanisms for cycling hypoxia imaging in vivo. Combining a luminescent ruthenium (II) complex (sensitizer) with a redox-active anthraquinone moiety (quencher), they developed a reversible two-photon luminescent probe to study cycling hypoxia in vivo using high-resolution spatial imaging. The quinone group was selected as the hypoxia-sensing moiety, and two-photon absorption of Ru^{2+} was obtained by using excitation wavelengths of 750–1050 nm, with an absorption peak at 800 nm and emission at 615 nm.

Nitroimidazoles

Apart from the aforementioned nitroimidazoles, Qian et al[59] developed nitroimidazoles as a dual-responsive nanocarrier, which was the first method that enhanced the traditional efficacy of PDT efficacy. This formulation comprised two components: reactive oxygen species (ROS)-generating and hypoxia-sensitive 2-nitroimidazole-grafted conjugated polymer (CP-NI), and encapsulated doxorubicin (designated DOX/CP-NI NPs). The nanocarrier complex could generate ROS after a light-triggered stimulus to release the hypoxia-responsive drug. The whole process is initiated with light irradiation, which leads to the generation of ROS and subsequently induces hypoxia at the tumor site by converting 2-nitroimidazole into hydrophilic 2-aminoimidazoles via a single-electron reduction

catalyzed by a series of nitroreductases coupled with bioreducing agents, such as NADPH, which eventually disassembles the drug carrier. The released doxorubicin can accumulate in cell nuclei to induce cytotoxicity via DNA damage, which is combined with the apoptotic effect of PDT to synergistically enhance antitumor activity. The strategy provides an innovative design guideline for stimuli-responsive drug delivery systems, which can undergo a series of programmed multiple triggers, in which one primary trigger activates the other trigger(s) to achieve synergistic treatment efficacy.

Aliphatic N-oxide

The prodrug AQ4N has a bis-N-oxide quinone structure that undergoes bioreduction in hypoxic cells. AQ4N has been evaluated in three phase I and II clinical trials. Upon reduction by hemoproteins that include cytochrome P450 (POR)[60,61] and nitric oxide synthase (NOS),[62,63] the reduction product AQ4 displays high DNA affinity by targeting topoisomerase II, which is crucial for cell division. The inhibition of topoisomerase II prevents hypoxic cells from reentering the cell cycle (Figure 2B). Although AQ4N itself has very little normal tissue toxicity and is considered an ideal bioreductive drug that can penetrate deep into the tumor tissue. Chemotherapeutic agents combined with AQ4N generally have high side effects, thereby hindering their clinical applications. Loading AQ4N into nano-carriers is an alternative method to overcome these problems. Knox et al[58] described Hypoxia Probe 1 (HyP-1), a hypoxia-responsive agent for photoacoustic imaging. HyP-1 is very select for hypoxic activation in vitro, in cultured cells, and in multiple disease models in vivo. The design of HyP-1 relies primarily on competitive binding with oxygen, rather than oxygen-dependent redox cycling. Minimal background results due to its action on oxygen-independent reduction pathways.[62] The authors demonstrated that photoacoustic imaging with HyP-1 enables three-dimensional visualization of intratumoral hypoxia with excellent resolution. Comparison of photoacoustic images acquired before and after HyP-1 administration revealed specific regions of signal enhancement, which were proposed to be correlated to regions of the most severe hypoxia. The superior resolution and imaging depth of photoacoustic images compared to fluorescence images indicated a promising outlook for this emerging imaging modality. Knox et al also established a hind limb ischemia model to evaluate the response of HyP-1 in hypoxic conditions in vivo, independent of extensive changes in gene and protein expression levels that can result from prolonged hypoxia in other models, such as cancer.[64,65]

In addition to the use of AQ4N in diagnosis, Feng et al[66] conceived an AQ4N-liposome-based nanodrug that relies on a commercial hydrophilic AQ4N molecule as the hypoxia-activated prodrug with a modified hydrophobic Ce6 (hCe6) as the photosensitizer that is simultaneously encapsulated into PEGylated liposomes. These liposomes may also be used as an imaging probe for positron emission tomography after chelation of the[62] Cu isotope, which has been demonstrated as an effective imaging probe for in vivo PET, in vivo fluorescence, photoacoustic imaging, PDT, and hypoxia-activated chemotherapy. AQ4N-hCe6 liposomes display obvious hypoxia-dependent cytotoxicity and effective photodynamic cell cytotoxicity. On the basis of these observations, Feng et al[69] used AQ4N in combination with glucose oxidase to achieve a combined cancer starvation and hypoxia-activated therapy. Glucose oxidase loaded into stealth liposomes can specifically block the glucose supply to a tumor, exhaust tumor oxygen to produce a hypoxic enhancement, and produce toxic hydrogen peroxide inside the tumors. Further treatment with stealth liposomes loaded with AQ4N demonstrated enhanced activation of hypoxia and strong synergistic antitumor effects.

Benzotriazine-N-oxide

Tirapazamine (TPZ), an aromatic N-oxide that was originally developed in the mid-1980s, has been the most extensively evaluated compound in clinics to date.[67] TPZ has 300-fold higher toxicity under anoxic conditions than under aerobic conditions.[68] TPZ can be reduced by one-electron reductases, such as P450 oxidoreductase, to a TPZ radical in the absence of oxygen. The TPZ radical undergoes spontaneous conversion to generate the benzotriazinyl radical that leads to DNA double-strand breaks, single-strand breaks, and DNA base damage (Figure 2C).[69,70] In addition to the one-electron reduction of TPZ, two-electron reduction has also been reported by enzymes, such as NQO1.[71] Two-electron reduction of TPZ has a bioprotective role in cells, because it bypasses formation of the TPZ radical to generate the mono N-oxide, a relatively non-toxic metabolite. TPZ has been evaluated in phase III clinical trials as a chemotherapy regimen in comparison with cisplatin and radiation therapy. Like other agents, cytotoxicity is a drawback for TPZ. Wang et al[72] developed iRGD peptide-modified nanoparticles loaded with indocyanine green and TPZ. Indocyanine green mediated PDT upon laser NIR

irradiation to induce hypoxia, which activated antitumor activity of the co-delivered TPZ for a synergistic cell killing effect. Guo et al[73] also developed an angiogenesis vessel-targeting nanoparticle (AVT-NP) consisting of a photosensitizer, angiogenic vessel-targeting peptide, and bioreductive prodrug for synergistic chemo-photo cancer therapy. The anticancer effect was first achieved by PDT, followed immediately by the generation of hypoxia-activated cytotoxic free radicals. The angiogenesis promoted by hypoxia could lead to the accumulation of AVT-NPs at the tumor site. PDT induces AVT-NPs accumulation at the tumor site due to enhanced angiogenesis in response to PDT-induced hypoxia. Hence, PDT can potentially enhance nanodrug accumulation at the tumor-stromal interface due to enhanced angiogenesis in response to PDT-induced hypoxia, resulting in higher efficacy. Increased hypoxia can achieve highly reactive TPZ radical formation from TPZ, eventually leading to a strong antitumor effect. This collaborative magnification was also observed by Liu et al[74] who reported the development of a nanocomposite combined PDT with hypoxia-activated chemotherapy using metal-organic framework and Hf-porphyrin synthesized Hf-porphyrin metal-organic framework platform (Hf-TCPP), with high porphyrin loading capacity. TPZ was inserted into the Hf-TCPP framework. The nanoplatform efficiently produced ROS for PDT upon irradiation. Furthermore, the depletion of oxygen aggravated the hypoxic environment of tumors to induce the activation of TPZ to enhance treatment efficacy. Apart from the aforementioned PDT-induced nanoparticles, Zhao et al[75] constructed PL-W18O49-TPZ, which combined PDT and photothermal therapy with hypoxia-activated chemotherapy, effective PET imaging properties and deeper skin penetration with a 808 nm laser. This was the first attempt at using the core W18O49 structure to create a more hypoxic tumor microenvironment and facilitate the activity of TPZ upon irradiation using a longer wavelength laser at 808 nm. Hypoxia-activated chemotherapy and photothermal therapy were simultaneously achieved for PL-W18O49-TPZ nanoparticles. Feng et al[79] reported the development of an ultrasound-mediated sequential hypoxia-specific nanotheranostics agent, TPZ/HMTNPs-SNO, which was generated by loading TPZ into hollow mesoporous titanium dioxide nanoparticles (HMTNPs) with modification of the S-nitrosothiol (SNO) moiety. The HMTNPs could function as sonosensitizers to generate ROS through the consumption of O_2 for sonodynamic therapy, which further sensitized the release of nitric oxide from SNO. Nitric oxide can be used as an ultrasound contrast agent to enhance ultrasound imaging. The activated TPZ could have a hypoxia-specific therapeutic effect.[76]

Azobenzoic-containing nanoparticles

Many researchers have used azobenzene for nanodrug loading. For example, Lee et al[77] reported a hypoxia/quinone oxidoreductase 1 (NQO1)-responsive doxorubicin delivery system, using mesoporous silica nanoparticles containing a surface cyclodextrin as a gatekeeper connected via an azobenzene linker (Si-Azo-CD-PEG) for hypoxic cancer-targeting drug delivery. Azobenzene can be effectively linked to the mesoporous silica nanoparticles and cyclodextrin, respectively. NQO1 is a cytosolic reductase that is upregulated in hypoxic cancer cells as a key stimulus for the selective cleavage of an azobenzene stalk, which triggers the gatekeeping switch for the controlled release of guest drugs. Activation of NQO1 can abrogate azobenzene binding, eliminating the gatekeeper and allowing unloading of the drug. Wang et al[78] developed a theranostic nanocarrier to integrate PDT and chemotherapy (Ce6-PEG-Azo-PCL) that was loaded with doxorubicin. The system has three primary constituents: a hypoxia-induced cleaved azobenzene bridge to sense hypoxia microenvironment, biodegradable hydrophobic poly(ε-caprolactone) as a hydrophobic segment, and hydrophilic poly(ethylene glycol)-decorated photosensitizer chlorine e6 (Ce6) to enhance loading content and minimize the premature release of Ce6 (Figure 4). Initially, the Ce6 photosensitizer is activated to generate ROS and a hypoxic microenvironment after irradiation. The hypoxia-responsive azobenzene is triggered for the stepwise reduction by reductases to aniline derivatives in the oxygen-deficient environment. After activation of the primary trigger, the release of anticancer drugs from the complex is triggered at the tumor. The tumor cells undergo apoptosis triggered by the presence of ROS and doxorubicin. A similar study was conducted by Zhang et al who constructed azobenzene containing conjugated polymer-based nanocarriers (CPs-CPT-Ce6 NPs) for use in combination PDT-chemotherapy.[79] The specificity and potency of small interfering RNA (siRNA) regulation of gene expression hold great promise for cancer therapy.[80] The first human phase I clinical trial in this area demonstrated that targeted siRNA delivery could systemically administer the specific gene inhibition (reduction in mRNA and protein) agents with an RNA interference-based mechanism of action.[81] Perche et al documented the first example of a hypoxia-induced nanocarrier for delivery of siRNA. The

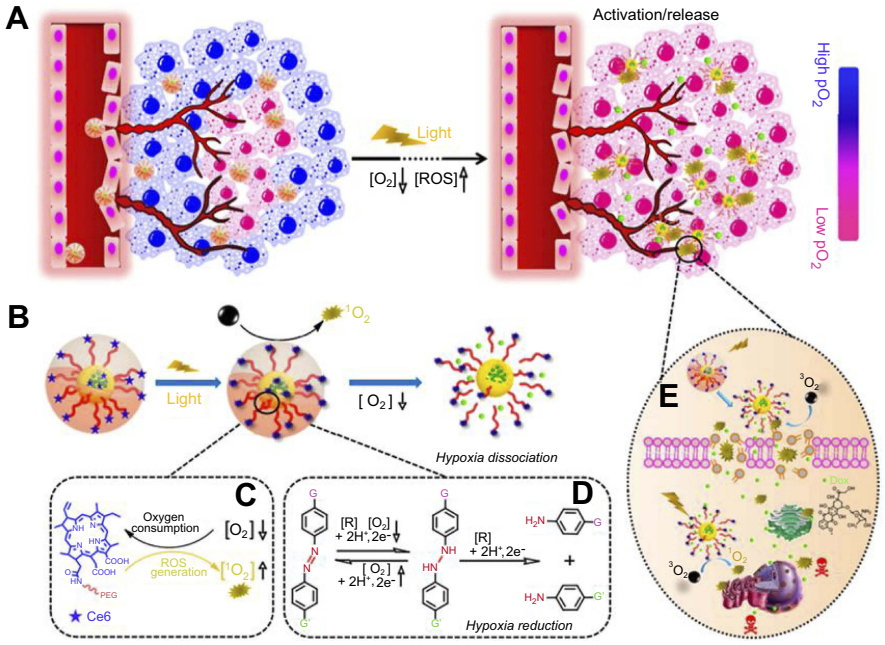

Figure 4 (**A**) Schematic of how the light-activated Dox@NP nanoparticles worked in combined combining hypoxia-triggered and PDT treatment strategy. (**B**) Generation of the ROS and hypoxia-induced disassembly upon laser irradiation. The mechanism of (**C**) photosensitized reaction induced by Ce6 and (**D**) stepwise reduction of azobenzene in hypoxia environment9. (**E**) light-driven synergistic therapy of ROS and Dox-based chemotherapy.

nanocarrier consisted of polyethyleneglycol (PEG), azobenzene (AZO), polyethyleneimine (PEI), and 1,2-dioleoyl-sn-glycero-3-phosphoethanolamine (DOPE) units (PEG-AZO-PEI-DOPE, collectively abbreviated PAPD). Within the PAPD, siRNA condensed into nanoparticles with a PEG layer to protect the siRNAs from nuclease attack and also to impart stability in physiological fluids.[82,83] PEG groups would detach from the PAPD/siRNA complexes under hypoxic conditions in the tumor environment by the degradation of the azobenzene linker by reductive enzymes. The positively charged PEI and the remaining PEI–DOPE/siRNA complexes could be easily taken up by the cells.[84] This strategy represented the first utilization of a hypoxia-activated siRNA nanocarrier to achieve gene silencing in vivo. However, the larger size of these compounds could limit intracellular aggregation.[85] Enhancement of the efficiency of intratumoral penetration of nanoparticles could possibly improve their treatment effect.[86] Particle sizes less than 10 to 20 nm[87] displayed better penetrating efficiency, but they might be rapidly cleared from the body through renal filtration.[88] Thus, an ideal nanoparticle should be relatively large in the blood circulation to prevent the renal filtration to achieve tumor-specific delivery through the enhanced permeability and retention effect and transform into small particles to penetrate into tumors once inside the tumor microenvironment. Xie et al[89] developed the first hypoxia-activated nanoparticles capable of decreased size for the co-delivery of doxorubicin and siRNA. Polyamidoamine (PAMAM) dendrimer was conjugated to PEG-2000 using the AZO hypoxia-sensitive to form PAMAM-AZO-PEG (collectively abbreviated PAP). Doxorubicin was loaded in the hydrophobic core of PAMAM, and HIF-1α siRNA (si-HIF) was bound to the surface of PAMAM through electrostatic forces between anionic siRNA and cationic primary amine groups (PAP +DOX+si-HIF). HIF-1α is a key transcriptional factor that activates a wide range of genes that regulate tumorigenesis, proliferation, and drug resistance.[90] The si-HIF is predictably effective and shows stronger tumor-suppressive effects. PAP was employed to co-deliver doxorubicin and si-HIF to tumors with the aim of enhancing the penetration of doxorubicin deep within tumors, simultaneously silence the expression of HIF-1α, and subsequently disturb crucial pathways of cancer development induced by hypoxia, as well as to reverse the drug resistance of tumor cells. Lu et al[91] reported a hypoxia- and pH-responsive and traceable co-delivery system for glioblastoma multiforme therapy. This multifunctional co-delivery system was constructed by assembling superparamagnetic iron oxide nanocubes for enhanced T2-weighted magnetic resonance imaging to trace the accumulation of nanoparticles that targeted ligand, and a peptide motif B6 was capable of crossing the blood–brain barrier, hypoxia responsive AZO, pH-responsive poly β-amino ester, and all-trans retinoic acid to induce the

differentiation glioblastoma stem cells to glioblastoma cells, and doxorubicin to regulate the intrinsic chemoresistance. This co-delivery system containing the AZO bond is rapidly broken in glioblastoma stem cells under hypoxic condition and subsequently triggers the release of all-trans retinoic acid and doxorubicin in the cells to synergistically kill the cancer cells. With spatiotemporal ability, the complex was able to overcome the issues of using doxorubicin for glioblastoma multiforme therapy and significantly improved the cytotoxicity of doxorubicin for glioblastoma cells and glioblastoma stem cells in vitro and in vivo. This approach has great potential for therapy of glioblastoma multiforme.[92]

Pt(IV)

Relative to their Pt(II) congeners, Pt(IV) complexes are relatively non-toxic. Pt(IV) complexes can be activated by either reducing agents or by ultraviolet irradiation to transform Pt(IV) into active Pt(II) metabolites by the loss of both axial ligands. The reduction process can be cytotoxic through the binding to nuclear DNA. As Pt(IV) is reduced to a lower oxidation state, similar radicals and ROS with higher oxidation states can be generated as a balance, without the consumption of endogenous oxygen. The reduced Pt(II) species and in situ self-generated ROS may function as effective cell killing agents for a combinatorial chemotherapy and PDT. Taking advantage of this property, Guo et al[93] synthesized a Pt(IV) complex-based prodrug monomer, which could be reduced to Pt(II) species to generate ROS in an O_2-independent manner. This could overcome the hypoxia existing in conventional PDT. To target deliver the drug to tumor site, 2-methacryloyloxyethyl phosphorylcholine monomer was employed to generate a polyprodrug with excellent solubility and increase its blood circulation time. The polyprodrug monomer exhibited combined chemotherapy and PDT efficacy against tumors.

Co(III)

Apart from the aforementioned use of Co(III) as fluorescence nanoparticles, the combination of chemotherapy drugs with Co(III) complexes is a promising strategy. Coordination of anticancer agents to Co(III) can inhibit the cytotoxic properties of the agents. When reduced to Co (II) in a hypoxic environment, the active molecule is released and restored to its active form to kill the surrounding cells. For example, Denny et al summarized a series of Co(III) complex in there report.[94] Three recently designed Co(III)-triazole complexes with structural and redox properties proved suitable for hypoxia-activated drug delivery, with structural and redox properties that were suitable for hypoxia-activated drug delivery.[95] Besides, Anna et al[96] present a bioreductively activated cobalt(III) carrier system for the delivery of curcumin with enhanced drug stability, tumor penetration, and efficacy in hypoxic tumor regions. Using a combination of fluorescence lifetime imaging and X-ray absorption spectroscopy to monitor the curcumin release.

Target HIF-1a and its derivative

HIF-1 induces the upregulation of glycolysis, which causes the accumulation of lactate, and many other substances, among them carbonic anhydrase IX (CA IX), a transmembrane protein neutralizing intracellular acidosis and of imparting chemoresistance, is a typical example.[97] There are two mechanisms to cause chemoresistance. First, chemotherapy can induce intracellular acidification, while CA IX prevents apoptosis by maintaining a normal intracellular pH against chemotherapy. Second, CA IX converts CO_2 and H_2O to H^+ and HCO_3^- in the extracellular space, which induces intracellular alkalosis through the bicarbonate transporter and H+ induced extracellular acidosis in the extracellular space, which is responsible for chemoresistance of cancer cells. Thus, HIF-1a and CA IX are associated with the killing of hypoxic tumors. Lots of clinical trials are underway to target CA IX. The trials are taking advantage of the fact that CA IX is not expressed in the majority of normal tissues and is strongly expressed in tumors. Therefore, inhibiting CA IX activity by binding to its active site or near can compromise the catalytic function of CA IX. Using specific monoclonal antibodies can enable the detection and killing of tumor cells that express CA IX.[98] A fluorescein isothiocyanate-conjugated carbonic anhydrase inhibitor thioureido-homosulfanilamide can reduce the extracellular acidification and bind only to hypoxic cells expressing CA IX. The result shows that there is no binding to CA IX-positive normoxic cells or CA IX-negative controls. Selective binding of conjugated inhibitor to CA IX-expressing hypoxic cells suggests that labeled CA IX inhibitors can be potentially used as tools for in vivo imaging of hypoxic tumors.[99] Alsaab et al[100] developed a simple and efficient multistage nanoplatform (ATZ-C4.16) for the systematic targeting of hypoxic environments to induce the combination of chemotherapeutic and immunotherapeutic effect in renal cell carcinoma. In this research, acetazolamide is the CA IX targeting agent, which

acts to improve tumor penetration compare to the nontargeted ligand in hypoxia. The cell division cycle and apoptosis regulator 1 protein analog (C4.16) as immunotherapeutic agent, which abolishes the activity of the phosphoinositide-3-kinase/protein kinase B pathway, triggers the pyrolysis of poly ADP ribose polymerase, downregulation of cyclin B, and upregulation of caspase-3 and −7. On the other hand, sorafenib acts as a chemotherapeutic agent by inhibiting VEGF receptor and BRAF. This comprehensive treatment can also upmodulate the tumoricidal function of M-1 macrophages and downmodulate tumorigenic M-2 macrophage-associated biomarkers, such as CD206 and arginase-1 by a mechanism that remains unclear. The combination of CA IX-C4.16 with sorafenib produced the targeted delivery of the payload in hypoxic tumors, resulting in induction of multimodal anticancer effects, including apoptosis, reversal of drug resistance, and reprogramming of malfunctioning macrophages.

Conclusion

Although the nanoparticle has been researched for decades. While the application of nanoparticle into clinical has rarely to be defined. The reason of it can be attributed to two part tumor part and nanoparticle part, as to tumor part tumor heterogeneity is one of the most important. The tumor heterogeneity lies in the different genetic mutations and the phenotypic expression profiles in genetic level, and complicated cell within the tumors, such as fibroblasts, other stromal cells, vascular cells, and infiltrating inflammatory cells (such as macrophages and lymphocytes) in cellular level. While their hypoxia active nanoparticle provides an important strategy to overcome the problem of tumor heterogeneity, which can be used to design diagnostic and therapeutic strategies for a broad range of solid tumors. As to the nanoparticle part, nanoparticle has many disadvantages such as poor tumor penetration on it large size, rapid renal clearance on its relative smaller size, scientist developed size shrinkable nanoparticle; the nanoparticle has short blood circulation time on its positive charge, easy to get through membrane on its positive charge, scientist developed nanoparticle with zero potential in its blood circulate period and can be positive charge after it activated by the hypoxia microenvironment. Based on the statement talked upon, the hypoxia active nanoparticle combined many merits. In recent years, we have seen great advances in the development of hypoxia active nanoparticles, which opened the door for better application of nanoparticles in tumor theranostics. We hope that this review helped to demonstrate the practical utility of hypoxia-active nanoparticle in delivery and that we will see further advancements toward clinical translation.

Acknowledgments

This work was supported by National Key R&D Program of China Grant under No.2017YFA0205200, 2018YFC0115500, The National Natural Science Foundation of China grant number [81630053], National Key R&D Program of China Grant under No. 2017YFA0700401, and The National Natural Science Foundation of China grant number [81227901, 81527805, 81501540, 61231004].

Disclosure

The authors report no conflicts of interest in this work.

References

1. Gatenby RA, Gillies RJ. A microenvironmental model of carcinogenesis. *Nat Rev Cancer*. 2008;8(1):56–61. doi:10.1038/nrc2255
2. Lewis DM, Park KM, Tang V, et al. Intratumoral oxygen gradients mediate sarcoma cell invasion. *Proc Natl Acad Sci U S A*. 2016;113(33):9292–9297. doi:10.1073/pnas.1605317113
3. Da Motta LL, Ledaki I, Purshouse K, et al. The BET inhibitor JQ1 selectively impairs tumour response to hypoxia and downregulates CA9 and angiogenesis in triple negative breast cancer. *Oncogene*. 2017;36(1):122–132. doi:10.1038/onc.2016.184
4. Chauhan VP, Jain RK. Strategies for advancing cancer nanomedicine. *Nat Mater*. 2013;12(11):958–962. doi:10.1038/nmat3792
5. Wilson WR, Hay MP. Targeting hypoxia in cancer therapy. *Nat Rev Cancer*. 2011;11(6):393–410. doi:10.1038/nrc3064
6. Bertout JA, Patel SA, Simon MC. The impact of O2 availability on human cancer. *Nat Rev Cancer*. 2008;8(12):967–975.
7. Cairns RA, Harris IS, Mak TW. Regulation of cancer cell metabolism. *Nat Rev Cancer*. 2011;11(2):85–95.
8. Vaupel P, Mayer A. Hypoxia in cancer: significance and impact on clinical outcome. *Cancer Metastasis Rev*. 2007;26(2):225–239.
9. Gilkes DM, Semenza GL, Wirtz D. Hypoxia and the extracellular matrix: drivers of tumour metastasis. *Nat Rev Cancer*. 2014;14(6):430–439. doi:10.1038/nrc3726
10. Harris AL. Hypoxia - A key regulatory factor in tumour growth. *Nat Rev Cancer*. 2002;2(1):38–47. doi:10.1038/nrc704
11. Keith B, Johnson RS, Simon MC. HIF1alpha and HIF2alpha: sibling rivalry in hypoxic tumour growth and progression. *Nat Rev Cancer*. 2011;12(1):9–22. doi:10.1038/nrc3183
12. Loscalzo J. Adaptions to hypoxia and redox stress: essential concepts confounded by misleading terminology. *Circ Res*. 2016;119(4):511–513. doi:10.1161/CIRCRESAHA.116.309394
13. Wardman P. Electron transfer and oxidative stress as key factors in the design of drugs selectively active in hypoxia. *Curr Med Chem*. 2001;8(7):739–761.
14. Schwartz HS, Sodergren JE, Philips FS. MITOMYCIN C: CHEMICAL AND BIOLOGICAL STUDIES ON ALKYLATION. *Science (New York, NY)*. 1963;142(3596):1181–1183. doi:10.1126/science.142.3596.1181

15. Iyer VN, Szybalski W. MITOMYCINS AND PORFIROMYCIN: CHEMICAL MECHANISM OF ACTIVATION AND CROSS-LINKING OF DNA. *Science (New York, NY)*. 1964;145 (3627):55–58. doi:10.1126/science.145.3627.55
16. Kumar R, Kim EJ, Han J, et al. Hypoxia-directed and activated theranostic agent: imaging and treatment of solid tumor. *Biomaterials*. 2016;104:119–128. doi:10.1016/j.biomaterials.2016.07.010
17. de Groot FM, Damen EW, Scheeren HW. Anticancer prodrugs for application in monotherapy: targeting hypoxia, tumor-associated enzymes, and receptors. *Curr Med Chem*. 2001;8(9):1093–1122.
18. Qiao Y, Wan J, Zhou L, et al. Stimuli-responsive nanotherapeutics for precision drug delivery and cancer therapy. *Wiley Interdiscip Rev Nanomed Nanobiotechnol*. 2018; 11(1). doi:10.1002/wnan.1527.
19. Sharma A, Arambula JF, Koo S, et al. Hypoxia-targeted drug delivery. *Chem Soc Rev*. 2019;48(3):771–813. doi:10.1039/c8cs00304a
20. Piao W, Hanaoka K, Fujisawa T, et al. Development of an azo-based photosensitizer activated under mild hypoxia for photodynamic therapy. *J Am Chem Soc*. 2017;139(39):13713–13719. doi:10.1021/jacs.7b05019
21. Yamamoto N, Renfrew AK, Kim BJ, Bryce NS, Hambley TW. Dual targeting of hypoxic and acidic tumor environments with a cobalt(III) chaperone complex. *J Med Chem*. 2012;55(24):11013–11021. doi:10.1021/jm3014713
22. Xie Z, Ma L, deKrafft KE, Jin A, Lin W. Porous phosphorescent coordination polymers for oxygen sensing. *J Am Chem Soc*. 2010;132(3):922–923. doi:10.1021/ja909629f
23. Finikova OS, Cheprakov AV, Vinogradov SA. Synthesis and luminescence of soluble meso-unsubstituted tetrabenzo- and tetranaphtho[2,3]porphyrins. *J Org Chem*. 2005;70(23):9562–9572. doi:10.1021/jo051580r
24. Neugebauer U, Pellegrin Y, Devocelle M, et al.Ruthenium polypyridyl peptide conjugates: membrane permeable probes for cellular imaging. *Chem Commun (Camb)*. 2008;(42):5307–5309. doi:10.1039/b810403d
25. Zhang S, Hosaka M, Yoshihara T, et al. Phosphorescent light-emitting iridium complexes serve as a hypoxia-sensing probe for tumor imaging in living animals. *Cancer Res*. 2010;70(11):4490–4498. doi:10.1158/0008-5472.CAN-09-3948
26. Tobita S, Yoshihara T. Intracellular and in vivo oxygen sensing using phosphorescent iridium(III) complexes. *Curr Opin Chem Biol*. 2016;33:39–45. doi:10.1016/j.cbpa.2016.05.017
27. Lv W, Yang T, Yu Q, et al. A phosphorescent iridium(III) complex-modified nanoprobe for hypoxia bioimaging via time-resolved luminescence microscopy. *Adv Sci (Weinh)*. 2015;2 (10):1500107. doi:10.1002/advs.201500088
28. Lv W, Zhang Z, Zhang KY, et al. A mitochondria-targeted photosensitizer showing improved photodynamic therapy effects under hypoxia. *Angew Chem Int Ed Engl*. 2016;55(34):9947–9951. doi:10.1002/anie.201604130
29. Feng Z, Tao P, Zou L, et al. Hyperbranched phosphorescent conjugated polymer dots with iridium(III) complex as the core for hypoxia imaging and photodynamic therapy. *ACS Appl Mater Interfaces*. 2017;9(34):28319–28330. doi:10.1021/acsami.7b09721
30. Zhu C, Liu L, Yang Q, Lv F, Wang S. Water-soluble conjugated polymers for imaging, diagnosis, and therapy. *Chem Rev*. 2012;112(8):4687–4735. doi:10.1021/cr200263w
31. Liu J, Liu Y, Bu W, et al. Ultrasensitive nanosensors based on upconversion nanoparticles for selective hypoxia imaging in vivo upon near-infrared excitation. *J Am Chem Soc*. 2014;136 (27):9701–9709. doi:10.1021/ja5042989
32. Papkovsky DB, Dmitriev RI. Biological detection by optical oxygen sensing. *Chem Soc Rev*. 2013;42(22):8700–8732. doi:10.1039/c3cs60131e
33. Weissleder R. A clearer vision for in vivo imaging. *Nat Biotechnol*. 2001;19(4):316–317. doi:10.1038/86684
34. Lv Z, Zou L, Wei H, Liu S, Huang W, Zhao Q. Phosphorescent starburst Pt(II) porphyrins as bifunctional therapeutic agents for tumor hypoxia imaging and photodynamic therapy. *ACS Appl Mater Interfaces*. 2018;10(23):19523–19533. doi:10.1021/acsami.8b05944
35. Zhao Q, Zhou X, Cao T, et al. Fluorescent/phosphorescent dual-emissive conjugated polymer dots for hypoxia bioimaging. *Chem Sci*. 2015;6(3):1825–1831. doi:10.1039/c4sc03062a
36. Zhou X, Liang H, Jiang P, et al. Multifunctional phosphorescent conjugated polymer dots for hypoxia imaging and photodynamic therapy of cancer cells. *Adv Sci (Weinh)*. 2016;3(2):1500155.
37. Fujibayashi Y, Taniuchi H, Yonekura Y, Ohtani H, Konishi J, Yokoyama A. Copper-62-ATSM: a new hypoxia imaging agent with high membrane permeability and low redox potential. *J Nucl Med*. 1997;38(7):1155–1160.
38. Lopci E, Grassi I, Rubello D, et al. Prognostic evaluation of disease outcome in solid tumors investigated with 64Cu-ATSM PET/CT. *Clin Nucl Med*. 2016;41(2):e87–e92. doi:10.1097/RLU.0000000000001017
39. Yu J, Zhang Y, Hu X, Wright G, Gu Z. Hypoxia-sensitive materials for biomedical applications. *Ann Biomed Eng*. 2016;44 (6):1931–1945. doi:10.1007/s10439-016-1578-6
40. Liu K, Zhu HL. Nitroimidazoles as anti-tumor agents. *Anticancer Agents Med Chem*. 2011;11(7):687–691. doi:10.2174/187152011796817664
41. Zbaida S, Levine WG. A novel application of cyclic voltammetry for direct investigation of metabolic intermediates in microsomal azo reduction. *Chem Res Toxicol*. 1991;4(1):82–88.
42. Nunn A, Linder K, Strauss HW. Nitroimidazoles and imaging hypoxia. *Eur J Nucl Med*. 1995;22(3):265–280.
43. Liu H, Xie Y, Zhang Y, et al. Development of a hypoxia-triggered and hypoxic radiosensitized liposome as a doxorubicin carrier to promote synergetic chemo-/radio-therapy for glioma. *Biomaterials*. 2017;121:130–143. doi:10.1016/j.biomaterials.2017.01.001
44. Spencer JA, Ferraro F, Roussakis E, et al. Direct measurement of local oxygen concentration in the bone marrow of live animals. *Nature*. 2014;508(7495):269–273. doi:10.1038/nature13034
45. Lin QN, Bao CY, Yang YL, et al. Highly discriminating photorelease of anticancer drugs based on hypoxia activatable phototrigger conjugated chitosan nanoparticles. *Adv Mater*. 2013;25 (14):1981–1986. doi:10.1002/adma.201204455
46. Liu F, Lou JZ, Hristov D. X-Ray responsive nanoparticles with triggered release of nitrite, a precursor of reactive nitrogen species, for enhanced cancer radiosensitization. *Nanoscale*. 2017;9 (38):14627–14634. doi:10.1039/c7nr04684g
47. Dobrowsky W, Huigol NG, Jayatilake RS, et al. AK-2123 (Sanazol) as a radiation sensitizer in the treatment of stage III cervical cancer: results of an IAEA multicentre randomised trial. *Radiother Oncol*. 2007;82(1):24–29. doi:10.1016/j.radonc.2006.11.007
48. Pasupathy K, Nair CK, Kagiya TV. Effect of a hypoxic radiosensitizer, AK 2123 (Sanazole), on yeast Saccharomyces cerevisiae. *J Radiat Res*. 2001;42(2):217–227.
49. Sreeja S, Krishnan Nair CK. Tumor control by hypoxia-specific chemotargeting of iron-oxide nanoparticle - Berberine complexes in a mouse model. *Life Sci*. 2018;195:71–80. doi:10.1016/j.lfs.2017.12.036
50. Sreeja S, Nair CKK. Chemo-directed specific targeting of nanoparticle-doxorubicin complexes to tumor in animal model. *J Drug Deliv Sci Technol*. 2016;31:167–175. doi:10.1016/j.jddst.2016.01.003
51. Erdogar N, Iskit AB, Eroglu H, Sargon MF, Mungan NA, Bilensoy E. Cationic core-shell nanoparticles for intravesical chemotherapy in tumor-induced rat model: safety and efficacy. *Int J Pharm*. 2014;471(1–2):1–9. doi:10.1016/j.ijpharm.2014.05.014

52. Carames Masana F, de Reijke TM. The efficacy of Apaziquone in the treatment of bladder cancer. *Expert Opin Pharmacother*. 2017;18(16):1781–1788. doi:10.1080/14656566.2017.1392510
53. Pierce SE, Guziec LJ, Guziec FS, Brodbelt JS. Characterization of aziridinylbenzoquinone DNA cross-links by liquid chromatography-infrared multiphoton dissociation-mass spectrometry. *Chem Res Toxicol*. 2010;23(6):1097–1104. doi:10.1021/tx1000738
54. Belcourt MF, Hodnick WF, Rockwell S, Sartorelli AC. Exploring the mechanistic aspects of mitomycin antibiotic bioactivation in Chinese hamster ovary cells overexpressing NADPH: cytochromeC (P-450) reductase and DT-diaphorase. *Adv Enzyme Regul*. 1998;38:111–133.
55. Rauth AM, Mohindra JK, Tannock IF. Activity of mitomycin C for aerobic and hypoxic cells in vitro and in vivo. *Cancer Res*. 1983;43(9):4154–4158.
56. Hou ZQ, Wei H, Wang Q, et al. New method to prepare mitomycin C Loaded PLA-nanoparticles with high drug entrapment efficiency. *Nanoscale Res Lett*. 2009;4(7):732–737. doi:10.1007/s11671-009-9312-z
57. Hou Z, Li Y, Huang Y, et al. Phytosomes loaded with mitomycin C-soybean phosphatidylcholine complex developed for drug delivery. *Mol Pharm*. 2013;10(1):90–101. doi:10.1021/mp300489p
58. Zhang P, Huang H, Chen Y, Wang J, Ji L, Chao H. Ruthenium(II) anthraquinone complexes as two-photon luminescent probes for cycling hypoxia imaging in vivo. *Biomaterials*. 2015;53:522–531. doi:10.1016/j.biomaterials.2015.02.126
59. Qian C, Yu J, Chen Y, et al. Light-activated hypoxia-responsive nanocarriers for enhanced anticancer therapy. *Adv Mater*. 2016;28(17):3313–3320. doi:10.1002/adma.201505869
60. McCarthy HO, Yakkundi A, McErlane V, et al. Bioreductive GDEPT using cytochrome P450 3A4 in combination with AQ4N. *Cancer Gene Ther*. 2003;10(1):40–48. doi:10.1038/sj.cgt.7700522
61. Nishida CR, Lee M, de Montellano PR. Efficient hypoxic activation of the anticancer agent AQ4N by CYP2S1 and CYP2W1. *Mol Pharmacol*. 2010;78(3):497–502. doi:10.1124/mol.110.065045
62. Nishida CR, Ortiz de Montellano PR. Reductive heme-dependent activation of the n-oxide prodrug AQ4N by nitric oxide synthase. *J Med Chem*. 2008;51(16):5118–5120. doi:10.1021/jm800496s
63. Mehibel M, Singh S, Chinje EC, Cowen RL, Stratford IJ. Effects of cytokine-induced macrophages on the response of tumor cells to banoxantrone (AQ4N). *Mol Cancer Ther*. 2009;8(5):1261–1269. doi:10.1158/1535-7163.MCT-08-0927
64. Paoni NF, Peale F, Wang F, et al. Time course of skeletal muscle repair and gene expression following acute hind limb ischemia in mice. *Physiol Genomics*. 2002;11(3):263–272. doi:10.1152/physiolgenomics.00110.2002
65. Knox HJ, Hedhli J, Kim TW, Khalili K, Dobrucki LW, Chan J. A bioreducible N-oxide-based probe for photoacoustic imaging of hypoxia. *Nat Commun*. 2017;8(1):1794. doi:10.1038/s41467-017-01951-0
66. Feng L, Cheng L, Dong Z, et al. Theranostic liposomes with hypoxia-activated prodrug to effectively destruct hypoxic tumors post-photodynamic therapy. *ACS Nano*. 2017;11(1):927–937.
67. Peters KB, Brown JM. Tirapazamine: a hypoxia-activated topoisomerase II poison. *Cancer Res*. 2002;62(18):5248–5253.
68. Zeman EM, Brown JM, Lemmon MJ, Hirst VK, Lee WW. SR-4233: a new bioreductive agent with high selective toxicity for hypoxic mammalian cells. *Int J Radiat Oncol Biol Phys*. 1986;12(7):1239–1242.
69. Shinde SS, Hay MP, Patterson AV, Denny WA, Anderson RF. Spin trapping of radicals other than the *OH radical upon reduction of the anticancer agent tirapazamine by cytochrome P450 reductase. *J Am Chem Soc*. 2009;131(40):14220–14221.
70. Delahoussaye YM, Evans JW, Brown JM. Metabolism of tirapazamine by multiple reductases in the nucleus. *Biochem Pharmacol*. 2001;62(9):1201–1209.
71. Patterson AV, Saunders MP, Chinje EC, Patterson LH, Stratford IJ. Enzymology of tirapazamine metabolism: a review. *Anticancer Drug Des*. 1998;13(6):541–573.
72. Wang Y, Xie Y, Li J, et al. Tumor-penetrating nanoparticles for enhanced anticancer activity of combined photodynamic and hypoxia-activated therapy. *ACS Nano*. 2017;11(2):2227–2238.
73. Guo D, Xu S, Wang N, et al. Prodrug-embedded angiogenic vessel-targeting nanoparticle: A positive feedback amplifier in hypoxia-induced chemo-photo therapy. *Biomaterials*. 2017;144:188–198.
74. Liu M, Wang L, Zheng X, Liu S, Xie Z. Hypoxia-triggered nanoscale metal-organic frameworks for enhanced anticancer activity. *ACS Appl Mater Interfaces*. 2018;10(29):24638–24647.
75. Zhao P, Ren S, Liu Y, Huang W, Zhang C, He J. PL-W18O49-TPZ nanoparticles for simultaneous hypoxia-activated chemotherapy and photothermal therapy. *ACS Appl Mater Interfaces*. 2018;10(4):3405–3413.
76. Feng Q, Li Y, Yang X, et al. Hypoxia-specific therapeutic agents delivery nanotheranostics: a sequential strategy for ultrasound mediated on-demand tritherapies and imaging of cancer. *J Control Release*. 2018;275:192–200.
77. Lee J, Oh ET, Yoon H, et al. Mesoporous nanocarriers with a stimulus-responsive cyclodextrin gatekeeper for targeting tumor hypoxia. *Nanoscale*. 2017;9(20):6901–6909.
78. Wang W, Lin L, Ma X, et al. Light-induced hypoxia-triggered living nanocarriers for synergistic cancer therapy. *ACS Appl Mater Interfaces*. 2018;10(23):19398–19407.
79. Zhang X, Wu M, Li J, et al. Light-enhanced hypoxia-response of conjugated polymer nanocarrier for successive synergistic photodynamic and chemo-therapy. *ACS Appl Mater Interfaces*. 2018;10(26):21909–21919.
80. Kim DH, Rossi JJ. Strategies for silencing human disease using RNA interference. *Nat Rev Genet*. 2007;8(3):173–184.
81. Davis ME, Zuckerman JE, Choi CHJ, et al. Evidence of RNAi in humans from systemically administered siRNA via targeted nanoparticles. *Nature*. 2010;464(7291):1067–U1140.
82. Ogris M, Brunner S, Schuller S, Kircheis R, Wagner E. PEGylated DNA/transferrin-PEI complexes: reduced interaction with blood components, extended circulation in blood and potential for systemic gene delivery. *Gene Ther*. 1999;6(4):595–605.
83. Takae S, Miyata K, Oba M, et al. PEG-detachable polyplex micelles based on disulfide-linked block catiomers as bioresponsive nonviral gene vectors. *J Am Chem Soc*. 2008;130(18):6001–6009.
84. Perche F, Biswas S, Wang T, Zhu L, Torchilin VP. Hypoxia-targeted siRNA delivery. *Angew Chem Int Ed Engl*. 2014;53(13):3362–3366.
85. Chauhan VP, Stylianopoulos T, Boucher Y, Jain RK. Delivery of molecular and nanoscale medicine to tumors: transport barriers and strategies. *Annu Rev Chem Biomol Eng*. 2011;2:281–298.
86. Waite CL, Roth CM. Nanoscale drug delivery systems for enhanced drug penetration into solid tumors: current progress and opportunities. *Crit Rev Biomed Eng*. 2012;40(1):21–41.
87. Prabhakar U, Maeda H, Jain RK, et al. Challenges and key considerations of the enhanced permeability and retention effect for nanomedicine drug delivery in oncology. *Cancer Res*. 2013;73(8):2412–2417.
88. Perrault SD, Walkey C, Jennings T, Fischer HC, Chan WC. Mediating tumor targeting efficiency of nanoparticles through design. *Nano Lett*. 2009;9(5):1909–1915.
89. Xie Z, Guo W, Guo N, et al. Targeting tumor hypoxia with stimulus-responsive nanocarriers in overcoming drug resistance and monitoring anticancer efficacy. *Acta Biomater*. 2018;71:351–362.

90. Semenza GL. Targeting HIF-1 for cancer therapy. *Nat Rev Cancer*. 2003;3(10):721–732.
91. Lu ZG, Li Y, Shi YJ, Li YH, Xiao ZB, Zhang X. Traceable nanoparticles with spatiotemporally controlled release ability for synergistic glioblastoma multiforme treatment. *Adv Funct Mater*. 2017;27(46):13.
92. Yang HY, Li Y, Lee DS. Multifunctional and stimuli-responsive magnetic nanoparticle-based delivery systems for biomedical applications. *Adv Ther*. 2018;1(2):1800011.
93. Guo D, Xu S, Huang Y, et al. Platinum(IV) complex-based two-in-one polyprodrug for a combinatorial chemo-photodynamic therapy. *Biomaterials*. 2018;177:67–77.
94. Denny WA, Wilson WR. Bioreducible mustards: a paradigm for hypoxia-selective prodrugs of diffusible cytotoxins (HPDCs). *Cancer Metastasis Rev*. 1993;12(2):135–151.
95. de Souza IC, Faro LV, Pinheiro CB, et al. Investigation of cobalt (iii)-triazole systems as prototypes for hypoxia-activated drug delivery. *Dalton Trans*. 2016;45(35):13671–13674.
96. Renfrew AK, Bryce NS, Hambley TW. Delivery and release of curcumin by a hypoxia-activated cobalt chaperone: a XANES and FLIM study. *Chem Sci*. 2013;4(9):3731–3739.
97. Sowa T, Menju T, Chen-Yoshikawa TF, et al. Hypoxia-inducible factor 1 promotes chemoresistance of lung cancer by inducing carbonic anhydrase IX expression. *Cancer Med*. 2017;6(1):288–297.
98. Pastorek J, Pastorekova S. Hypoxia-induced carbonic anhydrase IX as a target for cancer therapy: from biology to clinical use. *Semin Cancer Biol*. 2015;31:52–64. doi:10.1016/j.semcancer.2014.08.002
99. Dubois L, Douma K, Supuran CT, et al. Imaging the hypoxia surrogate marker CA IX requires expression and catalytic activity for binding fluorescent sulfonamide inhibitors. *Radiother Oncol*. 2007;83(3):367–373. doi:10.1016/j.radonc.2007.04.018
100. Alsaab HO, Sau S, Alzhrani RM, et al. Tumor hypoxia directed multimodal nanotherapy for overcoming drug resistance in renal cell carcinoma and reprogramming macrophages. *Biomaterials*. 2018;183:280–294. doi:10.1016/j.biomaterials.2018.08.053
101. Chen Y, Hu LQ. Design of Anticancer Prodrugs for Reductive Activation. *Med Res Rev*. 2009;29(1):29–64. doi:10.1002/med.20137
102. Phillips RM, Hendriks HR, Peters GJ. EO9 (Apaziquone): from the clinic to the laboratory and back again. *Br J Pharmacol*. 2013;168(1):11–18. doi:10.1111/j.1476-5381.2012.01996.x
103. Komatsu H, Tanabe K, Nishimoto S. C-13-labeled indolequinone-DTPA-Gd conjugate for NMR probing cytochrome: P450 reductase-mediated one-electron reduction. *Bioorg Med Chem Lett*. 2011;21(2):790–793. doi:10.1016/j.bmcl.2010.11.105
104. Nemeikaite-Ceniene A, Sarlauskas J, Anusevicius Z, Nivinskas H, Cenas N. Cytotoxicity of RH1 and related aziridinylbenzoquinones: involvement of activation by NAD(P)H: quinoneoxidoreductase (NQO1) and oxidative stress. *Arch Biochem Biophys*. 2003;416(1):110–118.
105. Yang YP, Kuo HS, Tsai HD, Peng YC, Lin YL. The p53-dependent apoptotic pathway of breast cancer cells (BC-M1) induced by the bis-type bioreductive compound aziridinylnaphthoquinone. *Breast Cancer Res*. 2005;7(1):R19–R27. doi:10.1186/bcr939
106. Li Y, Sun Y, Li J, et al. Ultrasensitive near-infrared fluorescence-enhanced probe for in vivo nitroreductase imaging. *J Am Chem Soc*. 2015;137(19):6407–6416. doi:10.1021/jacs.5b04097
107. Maurin MB, Rowe SM, Field KS, Swintosky RC, Hussain MA. Solubility behavior, phase transition, and structure-based nucleation inhibition of etanidazole in aqueous solutions. *Pharm Res*. 1996;13(9):1401–1405.
108. Bonnet M, Hong CR, Gu YC, et al. Novel nitroimidazole alkylsulfonamides as hypoxic cell radiosensitisers. *Bioorg Med Chem*. 2014;22(7):2123–2132. doi:10.1016/j.bmc.2014.02.039
109. Mallia MB, Mathur A, Sarma HD, Banerjee SA. (99m)Tc-labeled misonidazole analogue: step toward a (99m)Tc-alternative to [18F]fluromisonidazole for detecting tumor hypoxia. *Cancer Biother Radiopharm*. 2015;30(2):79–86. doi:10.1089/cbr.2014.1705
110. Aguilera KY, Brekken RA. Hypoxia Studies with Pimonidazole in vivo. *Bio-Protocol*. 2014;4:19. doi:10.21769/BioProtoc.1254
111. Zeng Y-C, Wu R, Xiao Y-P, et al. Radiation enhancing effects of sanazole and gemcitabine in hypoxic breast and cervical cancer cells in vitro. *Contemp Oncol (Pozn)*. 2015;19(3):236–240. doi:10.5114/wo.2015.51820
112. Hassan Metwally MA, Jansen JA, Overgaard J. Study of the population pharmacokinetic characteristics of nimorazole in head and neck cancer patients treated in the DAHANCA-5 trial. *Clin Oncol (R Coll Radiol)*. 2015;27(3):168–175. doi:10.1016/j.clon.2014.11.024
113. Metwally MA, Frederiksen KD, Overgaard J. Compliance and toxicity of the hypoxic radiosensitizer nimorazole in the treatment of patients with head and neck squamous cell carcinoma (HNSCC). *Acta Oncol*. 2014;53(5):654–661. doi:10.3109/0284186X.2013.864050
114. White CL, Menghistu T, Twigger KR, et al. Escherichia coli nitroreductase plus CB1954 enhances the effect of radiotherapy in vitro and in vivo. *Gene Ther*. 2008;15(6):424–433. doi:10.1038/sj.gt.3303081
115. Winters T, Sercel A, Suto C, et al. Design and synthesis of 2-nitroimidazoles with variable alkylating and acylating functionality. *Chem Pharm Bull*. 2014;62(3):301–303.
116. Hunter FW, Wouters BG, Wilson WR. Hypoxia-activated prodrugs: paths forward in the era of personalised medicine. *Br J Cancer*. 2016;114(10):1071–1077. doi:10.1038/bjc.2016.79
117. Baran N, Molecular Pathways: KM. Hypoxia-Activated Prodrugs in Cancer Therapy. *Clin Cancer Res*. 2017;23(10):2382–2390. doi:10.1158/1078-0432.CCR-16-0895
118. Takakusagi Y, Kishimoto S, Naz S, et al. Radiotherapy synergizes with the hypoxia-activated prodrug evofosfamide: in vitro and in vivo studies. *Antioxid Redox Signal*. 2018;28(2):131–140. doi:10.1089/ars.2017.7106
119. Patterson AV, Ferry DM, Edmunds SJ, et al. Mechanism of action and preclinical antitumor activity of the novel hypoxia-activated DNA cross-linking agent PR-104. *Clin Cancer Res*. 2007;13(13):3922–3932. doi:10.1158/1078-0432.CCR-07-0478
120. Guise CP, Abbattista MR, Singleton RS, et al. The bioreductive prodrug PR-104A is activated under aerobic conditions by human aldo-keto reductase 1C3. *Cancer Res*. 2010;70(4):1573–1584. doi:10.1158/0008-5472.CAN-09-3237
121. Kim EY, Liu Y, Akintujoye OM, et al. Preliminary studies with a new hypoxia-selective cytotoxin, KS119W, in vitro and in vivo. *Radiat Res*. 2012;178(3):126–137.
122. Penketh PG, Shyam K, Zhu R, Baumann RP, Ishiguro K, Sartorelli AC. Influence of phosphate and phosphoesters on the decomposition pathway of 1,2-bis(methylsulfonyl)-1-(2-chloroethyhydrazine (90CE), the active anticancer moiety generated by Laromustine, KS119, and KS119W. *Chem Res Toxicol*. 2014;27(5):818–833. doi:10.1021/tx500004y
123. Papadopoulou MV, Bloomer WD. NLCQ-1 (NSC 709257): exploiting hypoxia with a weak DNA-intercalating bioreductive drug. *Clin Cancer Res*. 2003;9(15):5714–5720.
124. Papadopoulou MV, Ji M, Rao MK, Bloomer WD. 4-3-(2-nitro-1-imidazolyl)propylamino −7-chloroquinoline hydrochloride (NLCQ-1), a novel bioreductive compound as a hypoxia-selective cytotoxin. *Oncol Res*. 2000;12(4):185–192.
125. Miller TJ, Schneider RJ, Miller JA, et al. Photoreceptor cell apoptosis induced by the 2-nitroimidazole radiosensitizer, CI-1010, is mediated by p53-linked activation of caspase-3. *Neurotoxicology*. 2006;27(1):44–59. doi:10.1016/j.neuro.2005.06.001

126. Breider MA, Pilcher GD, Graziano MJ, Gough AW. Retinal degeneration in rats induced by CI-1010, a 2-nitroimidazole radiosensitizer. *Toxicol Pathol*. 1998;26(2):234–239. doi:10.1177/019262339802600207
127. Sharma R, Sharma A. *2-Nitroimidazole as Potential Nanoprobe in Hypoxia Imaging by MRI/PET*. Boca Raton: Crc Press-Taylor & Francis Group; 2008.
128. Parkinson EI, Bair JS, Cismesia M, Hergenrother PJ. Efficient NQO1 substrates are potent and selective anticancer agents. *ACS Chem Biol*. 2013;8(10):2173–2183. doi:10.1021/cb4005832
129. Ger M, Kaupinis A, Nemeikaite-Ceniene A, et al. Quantitative proteomic analysis of anticancer drug RH1 resistance in liver carcinoma. *Biochim Biophys Acta*. 2016;1864(2):219–232. doi:10.1016/j.bbapap.2015.11.005
130. Celik A, Yetis G. An unusually cold active nitroreductase for prodrug activations. *Bioorg Med Chem*. 2012;20(11):3540–3550. doi:10.1016/j.bmc.2012.04.004
131. Jaberipour M, Vass SO, Guise CP, et al. Testing double mutants of the enzyme nitroreductase for enhanced cell sensitisation to prodrugs: effects of combining beneficial single mutations. *Biochem Pharmacol*. 2010;79(2):102–111. doi:10.1016/j.bcp.2009.07.025
132. Amaia A, Pachon G, Cascante M, Creppy EE, Monge A. Lopez de Cerain A. Selective toxicity of a quinoxaline 1,4-di-N-oxide derivative in human tumour cell lines. *Arzneimittel-Forschung*. 2005;55(3):177–182.
133. Gu Y, Jaiswal JK, Wang J, Hicks KO, Hay MP, Wilson WR. Photodegradation of the benzotriazine 1,4-Di-N-oxide hypoxia-activated prodrug SN30000 in aqueous solution. *J Pharm Sci*. 2014;103(11):3464–3472. doi:10.1002/jps.24099
134. Wang J, Guise CP, Dachs GU, et al. Identification of one-electron reductases that activate both the hypoxia prodrug SN30000 and diagnostic probe EF5. *Biochem Pharmacol*. 2014;91(4):436–446. doi:10.1016/j.bcp.2014.08.003
135. Hunter FW, Wang J, Patel R, et al. Homologous recombination repair-dependent cytotoxicity of the benzotriazine di-N-oxide CEN-209: comparison with other hypoxia-activated prodrugs. *Biochem Pharmacol*. 2012;83(5):574–585. doi:10.1016/j.bcp.2011.12.005
136. Wang J, Foehrenbacher A, Su J, et al. The 2-nitroimidazole EF5 is a biomarker for oxidoreductases that activate the bioreductive prodrug CEN-209 under hypoxia. *Clin Cancer Res*. 2012;18(6):1684–1695. doi:10.1158/1078-0432.CCR-11-2296
137. Hicks KO, Siim BG, Jaiswal JK, et al. Pharmacokinetic/pharmacodynamic modeling identifies SN30000 and SN29751 as tirapazamine analogues with improved tissue penetration and hypoxic cell killing in tumors. *Clin Cancer Res*. 2010;16(20):4946–4957. doi:10.1158/1078-0432.CCR-10-1439
138. Shen X, Laber CH, Sarkar U, et al. Exploiting the inherent photophysical properties of the major tirapazamine metabolite in the development of profluorescent substrates for enzymes that catalyze the bioreductive activation of hypoxia-selective anticancer Prodrugs. *J Org Chem*. 2018;83(6):3126–3131. doi:10.1021/acs.joc.7b03035
139. Manley E Jr., Waxman DJ. Impact of tumor blood flow modulation on tumor sensitivity to the bioreductive drug banoxantrone. *J Pharmacol Exp Ther*. 2013;344(2):368–377. doi:10.1124/jpet.112.200089
140. Nesbitt H, Byrne NM, Williams SN, et al. Targeting hypoxic prostate tumors using the novel hypoxia-activated prodrug OCT1002 inhibits expression of genes associated with malignant progression. *Clin Cancer Res*. 2017;23(7):1797–1808. doi:10.1158/1078-0432.CCR-16-1361
141. Failes TW, Cullinane C, Diakos CI, Yamamoto N, Lyons JG, Hambley TW. Studies of a cobalt(III) complex of the MMP inhibitor marimastat: A potential hypoxia-activated prodrug. *Chem Eur J*. 2007;13(10):2974–2982. doi:10.1002/chem.200601137
142. Schreiber-Brynzak E, Pichler V, Heffeter P, et al. Behavior of platinum(iv) complexes in models of tumor hypoxia: cytotoxicity, compound distribution and accumulation. *Metallomics*. 2016;8(4):422–433. doi:10.1039/c5mt00312a
143. Oszajca M, Collet G, Stochel G, Kieda C, Brindell M. Hypoxia-selective inhibition of angiogenesis development by NAMI-A analogues. *Biometals*. 2016;29(6):1035–1046. doi:10.1007/s10534-016-9974-9
144. Xie D, Kim S, Kohli V, et al. Hypoxia-responsive (19)F MRI probes with improved redox properties and biocompatibility. *Inorg Chem*. 2017;56(11):6429–6437. doi:10.1021/acs.inorgchem.7b00500